

Goniospectral Imaging of Three-Dimensional Objects*

Hideaki Haneishi,[▲] Takuya Iwanami, Tomoyuki Honma, Norimichi Tsumura,[▲] and Yoichi Miyake^{*}

Department of Information and Image Sciences, Chiba University, Inage-ku, Chiba, Japan

We propose a method for extracting goniospectral information of three-dimensional objects from multiband images obtained under several illuminants and reproducing the objects under various kinds of illuminants. Using the dichromatic reflection model, goniophotometric information of both diffuse component and specular component is estimated from the images acquired under the illuminant from several illumination directions. On the other hand, spectral information is estimated from five band images using the minimum mean square error criterion. Experimental results using simple three-dimensional objects are presented to demonstrate the basic performance of the proposed method.

Journal of Imaging Science and Technology 45: 451–456 (2001)

Introduction

In an electronic museum or Internet shopping, reproducing the color and glossiness of a three-dimensional (3-D) object with high fidelity is desired for observers or consumers to recognize more clearly what the object looks like. Spectral information is necessary for the exact representation of color objects and many researchers have conducted studies to obtain it.^{1–5} However, none of those studies have addressed the extraction of the characteristics necessary to reproduce the glossiness of the object.

For the reflection analysis of inhomogeneous dielectric objects, the dichromatic reflection model is usually used.⁶ In the model, the reflection of an object is composed of diffuse reflection (body reflection) and specular reflection (surface reflection). The perception of glossiness is basically induced by specular reflection from the object surface. Sato and Ikeuchi have proposed a method to extract the glossiness of a 3-D object.⁷ They acquired a sequence of images by changing the position of the light source while keeping the object and the camera position fixed. From the analysis of the sequence of images they have shown that the goniophotometric property can be extracted at each pixel in the image locally. However, their technique treats only a three-band image (red (R), green (G) and blue (B)) and is not sufficient for recovering spectral information.

We have proposed a basic idea for obtaining goniospectral information on an object, which has been

developed independently of that of Sato and Ikeuchi, but was found to be an extended version of their method.^{8,9} As shown in Fig. 1, light sources are located at several different positions while the 3-D object and the camera position are fixed. Multiband images are taken under the illumination from each light source. The images are then analyzed and the parameters representing goniospectral characteristics of the object are extracted and stored.

Once such information is obtained, we can estimate the spectral distribution at any point of an unoccluded surface of the object under an arbitrary spectral and spatial distribution of the light source and display its tristimulus values on a well-calibrated color CRT. Observers or consumers may enjoy the appearance of the object under a variety of light sources and then recognize the object's intrinsic color and surface characteristics more clearly.

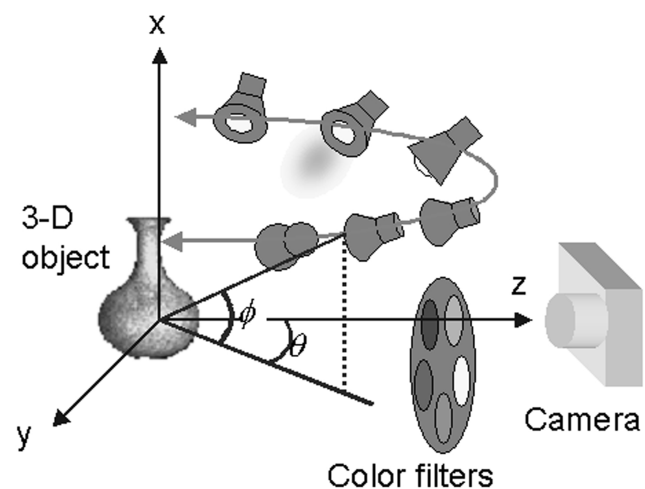


Figure 1. Multiangle illuminant, multiband imaging system.

Original manuscript received December 26, 2000

▲ IS&T Member

◆ IS&T Fellow

E-mail: haneishi@image.tp.chiba-u.ac.jp

* Presented in part at the IS&T/SID Sixth Color Imaging Conference and at IS&T's 2nd PICS Conference.

Color Plates 3 through 5 are printed in the color plate section of this issue, p. 483.

©2001, IS&T—The Society for Imaging Science and Technology

In this article, we describe details of the proposed method. In the following sections, the light reflection model is formulated and the factors that are required for reproduction simulation are described. Next, a multi-band image acquisition system is presented and the method of estimating the goniospectral factors of 3D objects is shown. The parametric representation of reproduction simulation is also shown. Then, the experiments that were conducted to validate the proposed method are presented.

Dichromatic Reflection Model

In this section, we first formulate a physical model of spectral light reflection from the object surface. Then, we show the factors that are required for the display simulation of the object under an arbitrary distribution of light source.

The coordinate system used in this study is shown in Fig. 1. We let column vector $\mathbf{f}(\mathbf{r};\theta,\phi)$ denote the spectral power distribution at position \mathbf{r} on the object surface when illumination was made from the direction of azimuth angle θ and elevation angle ϕ . According to the dichromatic reflection model, $\mathbf{f}(\mathbf{r};\theta,\phi)$ is denoted as the synthesis of the specular-reflection component, \mathbf{f}_s , and the diffuse-reflection component, \mathbf{f}_d :

$$\mathbf{f}(\mathbf{r};\theta,\phi) = \mathbf{f}_s(\mathbf{r};\theta,\phi) + \mathbf{f}_d(\mathbf{r};\theta,\phi). \quad (1)$$

We further assume that each component can be represented as

$$\mathbf{f}_s(\mathbf{r};\theta,\phi) = w_s(\mathbf{r};\theta,\phi)\mathbf{L}\mathbf{o}_w, \quad (2a)$$

$$\mathbf{f}_d(\mathbf{r};\theta,\phi) = w_d(\mathbf{r};\theta,\phi)\mathbf{L}\mathbf{o}(\mathbf{r}). \quad (2b)$$

Here, $w_s(\mathbf{r};\theta,\phi)$ and $w_d(\mathbf{r};\theta,\phi)$ denote the geometry-dependent factors of specular and diffuse components, respectively. \mathbf{L} is a diagonal matrix whose diagonal elements represent the spectral radiance of the illuminant. $\mathbf{o}(\mathbf{r})$ is a column vector representing the spectral reflectance of the object. On the other hand, \mathbf{o}_w is a column vector whose elements are all unity; consequently, $\mathbf{L}\mathbf{o}_w$ represents the spectral radiance equal to that of the illuminant. Thus, Eq. 2a means that the specular component is the same as the illuminant spectra in vector orientation.

Each term in Eq. 1 is expressed by a product of the normalized vector and the magnitude as shown in Eq. 3.

$$\mathbf{f}(\mathbf{r};\theta,\phi) = w_s^{(n)}(\mathbf{r};\theta,\phi)\mathbf{e}_s + w_d^{(n)}(\mathbf{r};\theta,\phi)\mathbf{e}_d(\mathbf{r}), \quad (3)$$

where

$$\mathbf{e}_s = \frac{\mathbf{L}\mathbf{o}_w}{\|\mathbf{L}\mathbf{o}_w\|}, \quad (4a)$$

$$\mathbf{e}_d(\mathbf{r}) = \frac{\mathbf{L}\mathbf{o}(\mathbf{r})}{\|\mathbf{L}\mathbf{o}(\mathbf{r})\|}, \quad (4b)$$

$$w_s^{(n)}(\mathbf{r};\theta,\phi) = w_s(\mathbf{r};\theta,\phi)\|\mathbf{L}\mathbf{o}_w\|, \quad (4c)$$

$$w_d^{(n)}(\mathbf{r};\theta,\phi) = w_d(\mathbf{r};\theta,\phi)\|\mathbf{L}\mathbf{o}(\mathbf{r})\|, \quad (4d)$$

What we want to determine are the four factors listed above, namely, (1) the unit vector \mathbf{e}_s that gives the spectral direction of the specular component and does not depend on the position \mathbf{r} , (2) the unit vector $\mathbf{e}_d(\mathbf{r})$ that gives the spectral direction of the diffuse component, (3) two scalar functions, $w_s^{(n)}(\mathbf{r};\theta,\phi)$ and $w_d^{(n)}(\mathbf{r};\theta,\phi)$, both of which depend on the geometry of the object surface and the illumination angle.

If these vectors and functions are obtained independently, one can simulate the appearance of the object under an arbitrary spectral distribution of light source with an arbitrary illumination angle by taking the following steps: 1) eliminating the illuminant used for image acquisition by multiplying the inverse of \mathbf{L} by the two unit vectors, 2) applying the illuminant for display simulation \mathbf{L}' , 3) multiplying the geometrical factor of each component at the new illumination angle (θ',ϕ') . These operations are expressed by the following equations:

$$w_s^{(n)}(\mathbf{r};\theta',\phi')\mathbf{L}'\mathbf{L}^{-1}\mathbf{e}_s = w_s(\mathbf{r};\theta',\phi')\mathbf{L}'\mathbf{o}_w, \quad (5a)$$

$$w_d^{(n)}(\mathbf{r};\theta',\phi')\mathbf{L}'\mathbf{L}^{-1}\mathbf{e}_d(\mathbf{r}) = w_d(\mathbf{r};\theta',\phi')\mathbf{L}'\mathbf{o}(\mathbf{r}). \quad (5b)$$

Finally, by synthesizing these two components, the object under such illumination can be simulated as

$$\hat{\mathbf{f}}(\mathbf{r};\mathbf{L}'(\theta',\phi')) = w_s(\mathbf{r};\theta',\phi')\mathbf{L}'(\theta',\phi')\mathbf{o}_w + w_d(\mathbf{r};\theta',\phi')\mathbf{L}'(\theta',\phi')\mathbf{o}(\mathbf{r}). \quad (6)$$

More generally, the arbitrary spatial distribution of the light source, say, a long fluorescent lamp, can be simulated as

$$\hat{\mathbf{f}}(\mathbf{r};\mathbf{L}'(\theta',\phi')) = \iint \{w_s(\mathbf{r};\theta',\phi')\mathbf{L}'(\theta',\phi')\mathbf{o}_w + w_d(\mathbf{r};\theta',\phi')\mathbf{L}'(\mathbf{r};\theta',\phi')\mathbf{o}(\mathbf{r})\}d\theta'd\phi'. \quad (7)$$

Here, $\mathbf{L}'(\mathbf{r};\theta',\phi')$ represents the spectral radiance of the illuminant to the direction of the object position \mathbf{r} at the illumination angle (θ',ϕ') . In the next section, we show how to estimate these four factors.

Method for Image Acquisition and Display Simulation

Multiband Image Acquisition System. Theoretically, two unit vectors, \mathbf{e}_s and \mathbf{e}_d have high dimensions (for instance, the dimension of the vectors is 81 when the optical wavelength range from 380 nm to 780 nm is sampled at 5 nm intervals) and two geometrical factors and $w_s^{(n)}$ and $w_d^{(n)}$ are the functions of two continuous variables, θ,ϕ . It is, however, not practical to capture many narrow-band images of the object under each of the densely spaced light sources to estimate these factors. Instead, we use sparsely located light sources for spatial sampling, and we use a limited number of spectral bands for spectral sampling. From such limited information, we estimate the goniospectral property under a light source with an arbitrary illumination angle and spectral distribution, based on the assumption that both characteristics have smooth variation.

Light sources of the imaging system are placed at several (N) different positions in order to cover the range of illumination angles expected in the display simulation. Each of the light sources illuminates a 3-D object by turn and its multiband images are captured

by a CCD camera with five color filters. The appropriate number of filters depends on the statistical distribution of the spectra of the target objects. Based on our experience in measuring the reflectance spectra of 147 oil paint color patches,³ we empirically decided to use five bands.

We denote the spectral radiance of the object under the i th light source with an illumination angle of $(\theta^{(i)}, \phi^{(i)})$ as

$$\begin{aligned} \mathbf{f}(\mathbf{r}; \theta^{(i)}, \phi^{(i)}) &= \mathbf{f}_s(\mathbf{r}; \theta^{(i)}, \phi^{(i)}) + \mathbf{f}_d(\mathbf{r}; \theta^{(i)}, \phi^{(i)}) \\ &= w_s(\mathbf{r}; \theta^{(i)}, \phi^{(i)}) \mathbf{Lo}_w + w_d(\mathbf{r}; \theta^{(i)}, \phi^{(i)}) \mathbf{Lo}(\mathbf{r}). \end{aligned} \quad (8)$$

The pixel value of the multiband image for this spectral radiance is expressed as

$$\begin{aligned} \mathbf{g}(\mathbf{r}; \theta^{(i)}, \phi^{(i)}) &= \mathbf{H} \mathbf{f}(\mathbf{r}; \theta^{(i)}, \phi^{(i)}) \\ &= w_s(\mathbf{r}; \theta^{(i)}, \phi^{(i)}) \mathbf{H} \mathbf{Lo}_w \\ &\quad + w_d(\mathbf{r}; \theta^{(i)}, \phi^{(i)}) \mathbf{H} \mathbf{Lo}(\mathbf{r}). \end{aligned} \quad (9)$$

Here, each row of matrix \mathbf{H} represents the overall spectral sensitivity of the camera with the corresponding filter, namely, this matrix transforms the spectral radiance of light to multiband pixel values.

The above equation is also expressed by using normalized vectors as

$$\begin{aligned} \mathbf{g}(\mathbf{r}; \theta^{(i)}, \phi^{(i)}) &= \\ w_s^{(n)}(\mathbf{r}; \theta^{(i)}, \phi^{(i)}) \mathbf{e}_w + w_d^{(n)}(\mathbf{r}; \theta^{(i)}, \phi^{(i)}) \mathbf{e}_d(\mathbf{r}). \end{aligned} \quad (10)$$

Here, we redefine the unit vectors as

$$\mathbf{e}_s = \frac{\mathbf{H} \mathbf{Lo}_w}{\|\mathbf{H} \mathbf{Lo}_w\|}, \quad (11a)$$

$$\mathbf{e}_d(\mathbf{r}) = \frac{\mathbf{H} \mathbf{Lo}(\mathbf{r})}{\|\mathbf{H} \mathbf{Lo}(\mathbf{r})\|}, \quad (11b)$$

$$w_s^{(n)}(\mathbf{r}; \theta^{(i)}, \phi^{(i)}) = w_s(\mathbf{r}; \theta^{(i)}, \phi^{(i)}) \|\mathbf{H} \mathbf{Lo}_w\|, \quad (11c)$$

$$w_d^{(n)}(\mathbf{r}; \theta^{(i)}, \phi^{(i)}) = w_d(\mathbf{r}; \theta^{(i)}, \phi^{(i)}) \|\mathbf{H} \mathbf{Lo}(\mathbf{r})\|. \quad (11d)$$

Unlike the cases of Eqs. 4 and 5, for the display simulation, the pseudoinverse of the matrix \mathbf{H} must be multiplied by two unit vectors prior to applying \mathbf{L}^{-1} .

How to Estimate Goniospectral Factors. Let us consider the behavior of pixel values at a certain pixel \mathbf{r} in the multiband images obtained. We denote the array of pixel values by vectors $\{\mathbf{g}(\mathbf{r}; \theta^{(i)}, \phi^{(i)})\}_{i=1, \dots, N}$. According to the dichromatic reflection model,⁶ these vectors approximately lie on a common plane spanned by the specular component vector and the diffuse component vector as formulated in Eq. 10. This property is schematically illustrated in Fig. 2. In this figure, dots represent the pixel value vectors $\{\mathbf{g}(\mathbf{r}; \theta^{(i)}, \phi^{(i)})\}_{i=1, \dots, N}$. Using this property, we determine the two unit vectors, then calculate the two geometrical functions as follows.

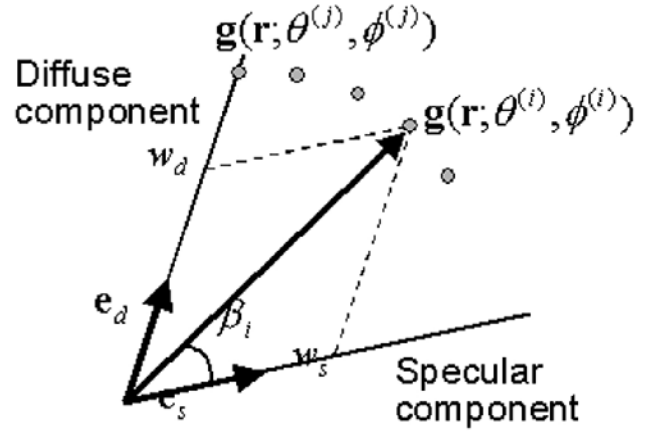


Figure 2. Schematic illustration of pixel values of multiband image based on the dichromatic reflection model.

(a) \mathbf{e}_s

We have used a reference white object (BaSO_4 plate) because its spectral reflectance is approximated by \mathbf{o}_w . By imaging it together with the target object and extracting its multiband pixel values, the direction of the illuminant spectrum can be estimated. The introduction of a white object is possible under our well-controlled imaging conditions. However, a more sophisticated method that does not require any reference white object may be used to simplify the preparation of the object.¹⁰

(b) $\mathbf{e}_d(\mathbf{r})$

If the illumination angle in the imaging system is varied widely, it is expected that there exists at least one illumination angle at which light from the object excludes the specular component almost completely. In the multiband vector space, such a vector should make its angle from the specular component, β maximum (vector $\mathbf{g}(\mathbf{r}; \theta^{(j)}, \phi^{(j)})$ in Fig. 2). Thus, if one finds such a vector and normalizes it as Eq. 12, it would be a unit vector of the diffuse component:

$$\mathbf{e}_d(\mathbf{r}) \equiv \left\{ \mathbf{g}(\mathbf{r}; \theta^{(i)}, \phi^{(i)}) / \left\| \mathbf{g}(\mathbf{r}; \theta^{(i)}, \phi^{(i)}) \right\| \middle| i = \arg \max_j \beta_j \right\}. \quad (12)$$

Practically, however, the vector array exhibits variation from the plane more or less due to noise, system instability and nonlinearity. Therefore, we first determine the plane that best fits the vector array by the least-squares method, then project each vector onto the plane. Subsequently, the vector that gives the maximum angle from the specular component is found and $\mathbf{e}_d(\mathbf{r})$ is calculated.

(c) Geometrical factors, $w_s^{(n)}(\mathbf{r}; \theta^{(i)}, \phi^{(i)})$, $w_d^{(n)}(\mathbf{r}; \theta^{(i)}, \phi^{(i)})$

Once unit vector \mathbf{e}_s and $\mathbf{e}_d(\mathbf{r})$ become known, two scalar $w_s^{(n)}(\mathbf{r}; \theta^{(i)}, \phi^{(i)})$ and $w_d^{(n)}(\mathbf{r}; \theta^{(i)}, \phi^{(i)})$ are obtained by solving Eq. 10.

Pseudo-Inverse of Matrix \mathbf{H} . In this study, we determine the inverse matrix \mathbf{H}^{-1} on the basis of minimum mean square error criterion using a set of color patches.^{3,11} The spectral radiance of each patch under the illuminant used for image acquisition is measured by a spectroradiometer, while the corresponding pixel values of multiband image are recorded by the multiband camera. Then, the inverse matrix \mathbf{H}^{-1} is given by

$$\mathbf{H}^- = \mathbf{F}\mathbf{G}^T(\mathbf{G}\mathbf{G}^T)^{-1}, \quad (13)$$

where \mathbf{F} is a matrix whose column is the spectral radiance of each color patch while \mathbf{G} is a matrix whose column is multiband pixel values of each color patch. $\mathbf{F}\mathbf{G}^T$ and $\mathbf{G}\mathbf{G}^T$ represent the correlation matrix between \mathbf{f} and \mathbf{g} , the autocorrelation matrix of \mathbf{g} , respectively. In our experiment, 24 color patches of the Macbeth color checker were used.

Approximation of Geometrical Factors Using Phong Model. In order to simulate arbitrary illumination angles, continuous functions, $w_s^{(n)}(\mathbf{r};\theta,\phi)$ and $w_d^{(n)}(\mathbf{r};\theta,\phi)$ are required rather than the discrete data sets $w_s^{(n)}(\mathbf{r};\theta^{(i)},\phi^{(i)})$ and $w_d^{(n)}(\mathbf{r};\theta^{(i)},\phi^{(i)})$. We model these components on the basis of Phong model¹² as

$$\begin{aligned} \hat{w}_s^{(n)}(\mathbf{r};\theta,\phi) = \\ A_s(\mathbf{r}) \cos^{\alpha(\mathbf{r})}(\theta - \theta_s(\mathbf{r})) \cos^{\alpha(\mathbf{r})}(\phi - \phi_s(\mathbf{r})), \end{aligned} \quad (14)$$

$$\begin{aligned} \hat{w}_d^{(n)}(\mathbf{r};\theta,\phi) = \\ A_d(\mathbf{r}) \cos(\theta - \theta_d(\mathbf{r})) \cos(\phi - \phi_d(\mathbf{r})). \end{aligned} \quad (15)$$

The model parameters $A_s(\mathbf{r})$, $\theta_s(\mathbf{r})$, $\phi_s(\mathbf{r})$, $\alpha(\mathbf{r})$, $A_d(\mathbf{r})$, $\theta_d(\mathbf{r})$, $\phi_d(\mathbf{r})$ are determined so that the approximated values best fit the data set, $\{w_s^{(n)}(\mathbf{r};\theta^{(i)},\phi^{(i)})\}$ and $\{w_d^{(n)}(\mathbf{r};\theta^{(i)},\phi^{(i)})\}$. A MATLAB optimization toolbox is used for this fitting. Note that in this model we assume that the object surface is isotropic.

Procedure for Image Display Simulation. The procedure for image display simulation is summarized by the following equation:

$$\begin{aligned} \mathbf{v}(\mathbf{r}, \mathbf{L}'(\theta', \phi')) = \\ \mathbf{T} \int \int w_s^{(n)}(\mathbf{r};\theta',\phi') \mathbf{L}'(\theta',\phi') \mathbf{L}^{-1} \mathbf{H}^- \cdot \frac{\mathbf{H}\mathbf{L}\mathbf{o}_w}{\|\mathbf{H}\mathbf{L}\mathbf{o}_w\|} d\theta' d\phi' \\ + \mathbf{T} \int \int w_d^{(n)}(\mathbf{r};\theta',\phi') \mathbf{L}'(\theta',\phi') \mathbf{L}^{-1} \mathbf{H}^- \cdot \frac{\mathbf{H}\mathbf{L}\mathbf{o}(\mathbf{r})}{\|\mathbf{H}\mathbf{L}\mathbf{o}(\mathbf{r})\|} d\theta' d\phi' \end{aligned} \quad (16)$$

Each operation in this equation is described below.

1. Multiply the pseudo-inverse, \mathbf{H}^- by the specular and diffuse unit vectors.
2. Multiply the inverse matrix \mathbf{L}^{-1} by both components to remove the effect of illuminant for image acquisition.
3. Multiply the new illuminant \mathbf{L}' by both components.
4. Multiply the geometrical factors w_s and w_d by the corresponding components, respectively.
5. If spatially broad light sources are simulated, repeat (1)-(4) for each light source position and take the summation (the integration in the above general form).
6. Multiply the color-matching functions, \mathbf{T} , of the calibrated CRT for display. Rows of \mathbf{T} represent red, green and blue color-matching function. Upon receiving this RGB signal, a well-calibrated CRT may produce tristimulus values that gives the same color as the object under the virtual illuminant.

If we take into account the effect of ambient light when watching the CRT, we must introduce further any color

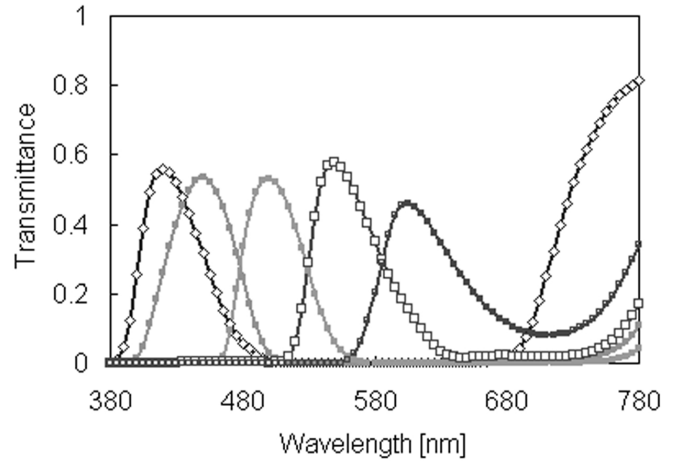


Figure 3. Spectral transmittance of five color filters used in the experiment.

appearance model into the above procedure.¹³ Such task is beyond the scope of this study. Note that our goal here is to reproduce the physical tristimulus values of the object under the virtual illuminant.

Experiment

Apparatus

Experiments of multiband-image acquisition and image display using simple dielectric objects were conducted to confirm the principle. **Color Plate 3 (p. 483)** shows the cylindrical objects, the Macbeth color checker and the reference white plate used in the experiments. This image is the one captured by a conventional digital camera. Two cylinders of different sizes have colored belts made of paper on their surfaces. The big cylinder has four belts with similarly weak glossiness but different colors. The small cylinder has 13 belts with different glossiness and different colors.

A 300W incandescent lamp was used as the illuminant in image acquisition. A cooled monochromatic CCD camera (MUTOH, CV04) with 16-bit quantization levels was used to achieve a wide dynamic range and avoid the saturation of pixel values in the glossy area. This camera has 384×256 pixel resolution. Five bandpass filters were arranged on a rotating wheel that was attached in front of the CCD camera and controlled by a PC. The five filters used had the following center wavelengths (FWHM in nm): 420(55), 450(60), 500(55), 550(55), and 600(70) nm. Figure 3 shows the spectral transmittances of these filters.

The distance between the light sources and the object was approximately 1.5m. Ten azimuth angles, $\theta = -50, -40, -30, -20, -10, 10, 20, 30, 40$, and 50 degrees, were used while the elevation angle ϕ was fixed to 0 degree. Zero degrees of azimuth angle was missing because the light source could not be placed there because of the camera. Captured images were processed by a Pentium 700MHz PC. All programs except for camera and filter control were coded in MATLAB.

Spectral Estimation

As described above, the inverse matrix \mathbf{H}^- for spectral estimation from the multiband image was determined using 24 color patches of the Macbeth checker. The spectral radiance of the 24 color patches under the incandescent lamp was measured by a

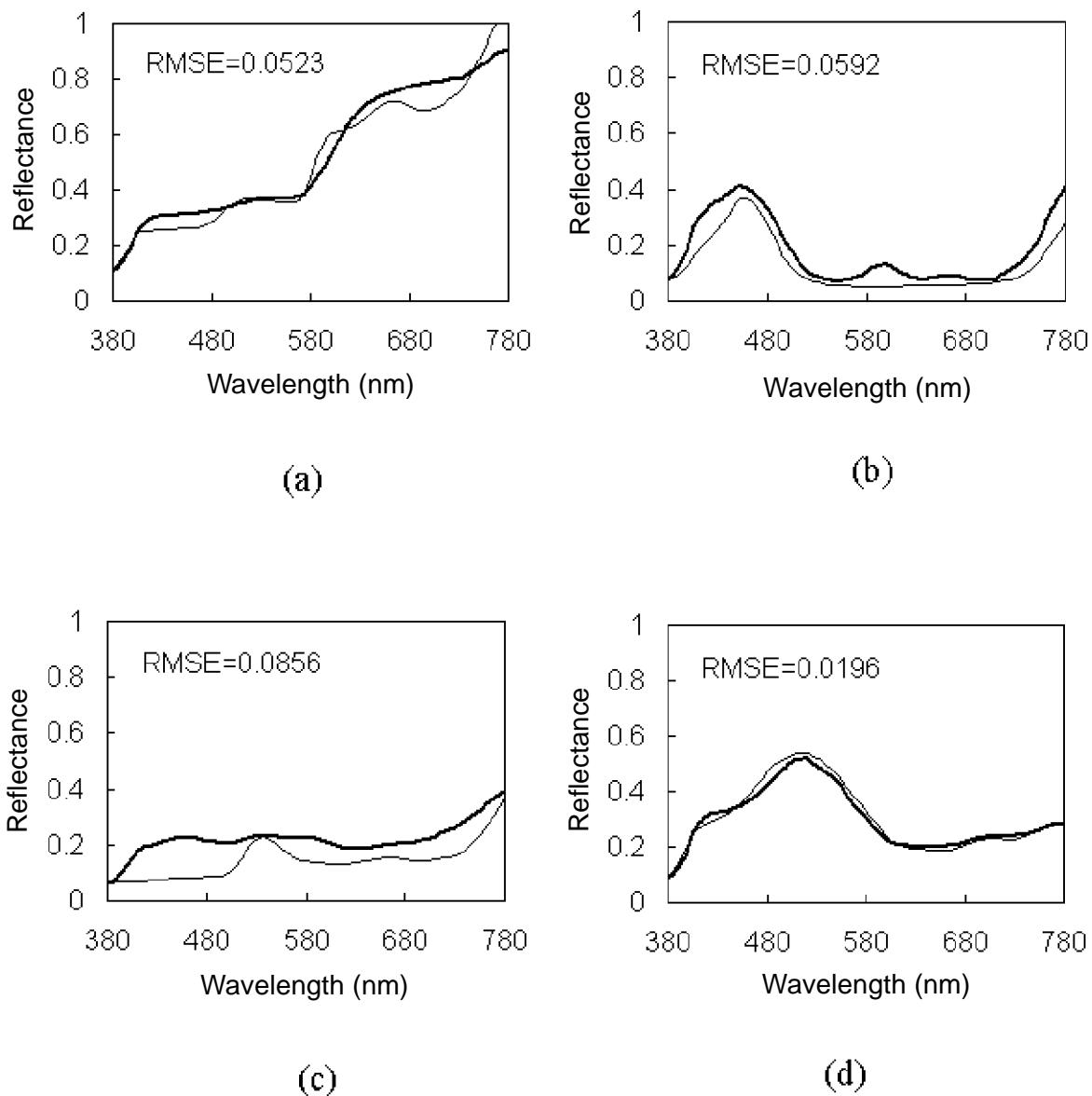


Figure 4. Comparison of measured (thin line) and estimated (thick line) spectral reflectances of the Macbeth color checker. (a) and (b) are examples with moderate accuracy, (c) is an example with poor accuracy and (d) is that with good accuracy.

spectroradiometer CS1000 (Minolta), while multiband images of the Macbeth checker were captured under the same conditions.

The accuracy of the spectral estimation was evaluated by the 24 color patches themselves. Spectral reflectance was calculated by dividing the spectral radiance of each patch by that of the reference white plate. The estimation error for each color patch was evaluated by the root-mean-square error (RMSE) defined by

$$RMSE = \sqrt{\frac{1}{n} \sum_{i=1}^n (o_i - \hat{o}_i)^2}.$$

Here, n is the number of sampling wavelengths and is 81 in this study. o_i and \hat{o}_i represent the measured and estimated reflectances at the i th wavelength, respectively. The average RMSE over 24 patches was 0.0576. The maximum and minimum RMSEs were 0.1209 and 0.0156,

respectively. Figure 4 shows a comparison between measured and estimated spectral reflectances of four patches. In this figure, (a) and (b) are examples with moderate accuracy, and (c) and (d) are those with poor and good accuracy, respectively. The RMSE values presented above and the graphical comparison shown in Fig. 4 indicate that the estimation accuracy is relatively good. However, further improvement is desired for more accurate color reproduction. If the target object is limited to a specific category, e.g., oil painting or cloth, the estimation accuracy may improve by calibrating with the samples belonging to the category.

Component Separation and Extraction of Geometrical Factors. From the obtained set of images, the model parameters described in the previous section were estimated. **Color Plate 4 (p. 483)** shows two separated component images obtained, assuming that the illuminant is an incandescent lamp and the illumination angle is $\theta = -30$ degrees. The intensity of the specular component image is slightly enhanced because the

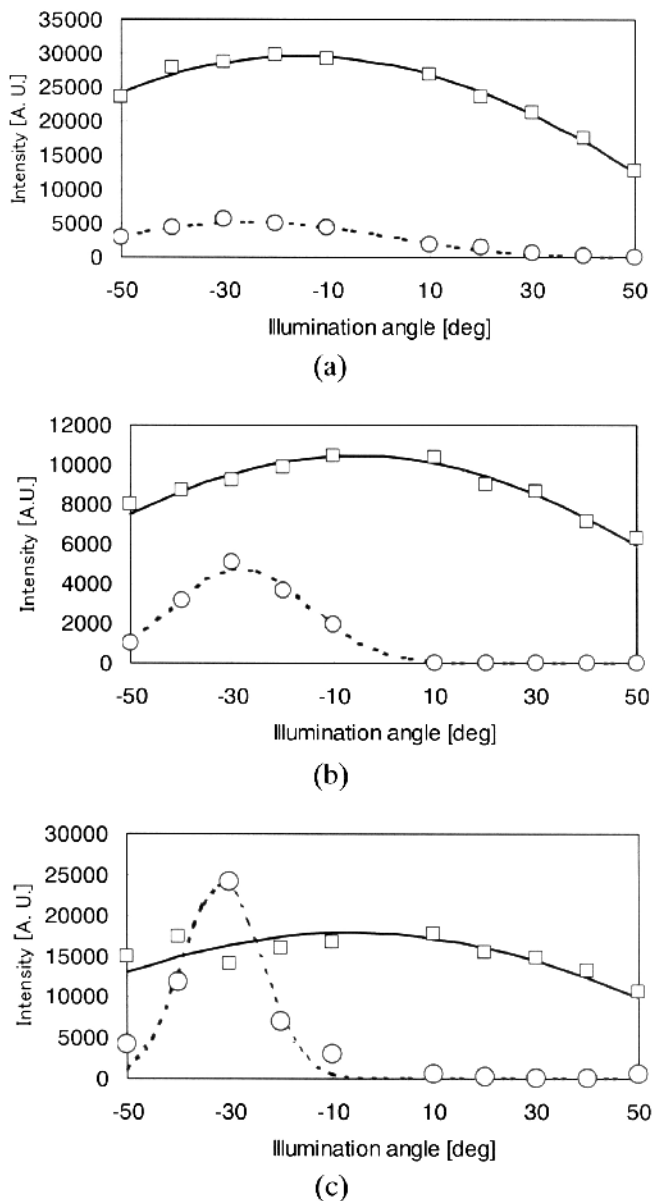


Figure 5. Variation of diffuse and specular components as the illumination angle changes.

true values are too small for visualization. It is seen that the two components are separated well except at some parts in the image. The highly glossy parts (bottom three belts of the small cylinder) are not successfully imaged. We consider that this is because the intense specular component affects the diffuse component in the presence of an even slight discrepancy between the model and the actual measurement.

The variation of geometrical factors, w_s and w_d , at three points on the objects as the illumination angle changes is demonstrated in Fig. 5. Note that these factors are the functions of only the azimuth angle θ because the elevation angle ϕ was fixed at 0 in this study. The graphs for three color belts with different glossiness are shown: (a) the less glossy red belt on top of the big cylinder, (b) the moderately glossy dark belt fifth from the bottom of the small cylinder, (c) the very glossy, bottommost orange belt of the small cylinder. The geometrical factors, w_s and w_d , extracted are plotted by circles and squares, respectively. It is clearly shown that

the three color belts with different glossiness give markedly different curves for the specular component. Solid and dashed lines represent fitted curves for diffuse and specular components, respectively. These curves fit the plots well though there is some error, particularly in the case with a strong specular component.


Demonstration of Image Display¹⁶

Once all the parameters of the object are obtained, the reproduction of the object under various kinds of illuminants is possible. Here, we demonstrate only two kinds of image display simulations. **Color Plate 5 (p. 483)** shows the simulated images of the object under the following illuminants:

- Illuminant is D65. Illumination angle is 35 degrees; this is not the angle used in image acquisition but is an interpolated one.
- Illuminant is D65. Illumination angle is broad, ranging from 0 to 50 degrees.

In **Color Plate 5a (p. 483)**, the interpolated image looks very natural because of the smooth property of the geometrical factors. In **Color Plate 5b (p. 483)**, it is seen that a spatially broad light source weakens the glossy appearance of the object.

Conclusions

A method for extracting goniospectral information of 3-D objects from five-band images obtained under several illuminants and reproducing the object under various kinds of illuminants has been proposed. In the estimation of spectral reflectance from five-band images, an RMSE of 0.0576 on average was achieved. However, further improvement is necessary for more accurate color reproduction. Experimental results using simple 3-D objects have successfully demonstrated the basic performance of the proposed method. For more realistic image display, however, we have to resolve many issues including the treatment of shadows, the examination of more suitable reflection models^{14,15} and so forth. 

Acknowledgment. This study was supported in part by a Grant-in-Aid for the Encouragement of Young Scientists, #11750035, from The Ministry of Education, Science and Sports and Culture of Japan.

References

- K. Martinez, J. Cupitt, and D. Saunders, *Proc. SPIE* **1901**, 25 (1993).
- H. Maitre, F. J. M. Schmitt, J. -P. Crettez, Y. Wu, and J. Y. Hardeberg, *Proc. IS&T/SID Fourth Color Imaging Conference*, IS&T, Springfield, VA, 1996, pp. 50-54.
- H. Haneishi, T. Hasegawa, N. Tsumura and Y. Miyake, *Appl. Opt.* **6621** (2000).
- F. Konig, *Proc. IS&T's 50th Annual Conference*, IS&T, Springfield, VA, 1997, pp. 454-458.
- F. H. Imai and R. S. Berns, *Proc. IS&T/SID Sixth Color Imaging Conference*, IS&T, Springfield, VA, 1998, pp. 224-229.
- S. Shafer, *Color Res. and Appl.*, **10**, 210 (1985).
- Y. Sato and K. Ikeuchi, *Graph. Mod. and Image Proc.* **58**, 437 (1996).
- H. Haneishi, T. Iwanami, T. Honma, N. Tsumura and Y. Miyake, *Proc. IS&T/SID's 6th Color Imaging Conference*, IS&T, Springfield, VA, 1998, pp. 173-176.
- H. Haneishi, T. Iwanami, T. Honma, N. Tsumura and Y. Miyake, *Proc. IS&T's PICS Conference*, IS&T, Springfield, VA, 1999, pp. 354-358.
- S. Tominaga, *J. Opt. Soc. Am.* **13**, 2163 (1996).
- W. K. Pratt, *Digital Image Processing*, 2nd ed., Wiley Interscience, New York (1991).
- B.-T. Phong, *Communications of the ACM* **18**, 311 (1975).
- K. M. Braun, and M. D. Fairchild, *Color Res. and Appl.* **22**, 165 (1997).
- S. Tominaga, *Color Res. and Appl.* **19**, 277 (1994).
- K. E. Torrance and E. M. Sparrow, *J. Opt. Soc. Amer.* **57**, 1105 (1967).
- Many simulated images including animation simulating a moving light source are shown on our web page at <http://sawori.tp.chiba-u.ac.jp/~haneishi/goniodemo/index.htm>.